

# The PARSEC program: a large sample of brown dwarf trigonometric parallaxes

Alexandre H. Andrei,<sup>1†</sup> Richard L. Smart,<sup>2</sup> Beatrice Bucciarelli,<sup>2</sup>  
Jucira L. Penna,<sup>3</sup> Federico Marocco,<sup>4</sup> Mario G. Lattanzi,<sup>2</sup>  
Mariateresa Crosta,<sup>2</sup> and Ramakrishna Teixeira<sup>5</sup>

<sup>1</sup>Observatório Nacional/MCTI, Brazil; Osservatorio Astrofisico di Torino/INAF, Italy; SYRTE/Observatoire de Paris, France; Observatório do Valongo/UFRJ, Brazil  
email: oat1@on.br

<sup>2</sup>Osservatorio Astrofisico di Torino/INAF, Italy

<sup>3</sup>Observatório Nacional/MCTI, Brazil

<sup>4</sup>CAR/University of Hertfordshire, United Kingdom

<sup>5</sup>IAG/Universidade de São Paulo, Brazil

**Abstract.** We report on the PARSEC program, which observed 140 L and T dwarfs on a regular basis from 2007 to 2011, using the WFI camera on the ESO/2.2 m telescope. Trigonometric parallaxes at 5 mas precision are derived for 49 objects, and mas yr<sup>-1</sup>-level proper motions are derived for approximately 200,000 objects in the same fields. We discuss image cleaning, object centroiding, and astrometric methods, in particular three different approaches for trigonometric parallax determination.

**Keywords.** astrometry, stars: low-mass, brown dwarfs, stars: luminosity function

---

## 1. Program features

The PARSEC (Parallaxes of Southern Extremely Cool objects) program was initiated to address the lack of absolute distances in many of the brown dwarf (BD) subclasses. It measured trigonometric parallaxes of 122 L and 28 T dwarfs brighter than  $z = 20$  mag in the southern hemisphere, most of which will not be observed by *Gaia*. This represented a doubling of the number of L dwarfs with trigonometric parallaxes, and, combined with existing results, it left no spectral subclass—up to L9—with fewer than 10 members. Of the 140 targets, only 14 had less than 1 yr of observations; from class L0 to T7, no subclass had more than two members with less than 1 yr of observations. Interesting and/or benchmark objects were selected for spectroscopic observations, mostly obtained with *SOAR/Spartan* (Marocco *et al.* 2012), of which we show selected results.

The program started in 2007 and ended in early 2011, comprising 4 to 6 observation epochs (2 to 3 nights) per year. All observations were taken using the WFI camera on the 2.2 m telescope at ESO's La Silla Observatory, Chile. For each star, one initial short exposure (50 or 100 s, depending on magnitude) was performed to identify the target. We then used the move-to-pixel procedure to put the target on pixel (520, 520) of CCD#7, followed by two long-exposure (3× the short exposure time) images, which were used for our parallax determinations. The exposures were done in the  $z$  band as a compromise between optimum quantum efficiency in the  $I$  band and typical target brightness: ( $I - z$ )  $\approx 2$  mag. Although the WFI camera is characterized by significant distortions at mas

† Present address: Shanghai Astronomical Observatory, Chinese Academy of Sciences, Shanghai, China

level, stability and repeatability are the crucial requirements for relative astrometry and those were maintained throughout by enforcing the move-to-pixel procedure to attain repeatability. For parallax determinations, only the top one-third of CCD#7 was used, because it is close to the optical axis and, thus, a zone affected minimally by distortions. For a full account of the program's setup and procedures, see Andrei *et al.* (2011).

## 2. Astrometric and Parallax Methods

Image treatment starts with standard IRAF routines for bias and flat-field corrections, but fringing removal uses a tailored approach. The latter is based on the short-exposure images as well as a few (usually four) science frames, aligned and combined using their mode to remove stellar ghosts. The nightly fringe map is subtracted from each raw frame in two steps. First, the image contribution is scaled using the exposure time. Second, the mean image counts are used as scale factors.

Object matching is of central importance for a long-term program, not only to keep track of the numerous measurements of the same object, but also to select the best objects to use for combining images. The probability to correctly match one object in two frames is  $P = 1/(\Phi S)$ , where  $\Phi$  is the stellar density and  $S$  the frame size. Usual cone-search strategies run into trouble for long time intervals. We avoid such pitfalls by adopting the following strategy: (i) the matching goes hand in hand with the fitting process; (ii) we assign high orders in the matching process to objects without any proper motion between consecutive images, and low orders to unpaired objects; (iii) we use relative astrometry to a precision of better than 100 mas. Under those conditions  $P > 0.99$  already when a third night is added, even for  $\Phi = 1000 \text{ deg}^{-2}$ ; (iv) we remove the stars matched in the previous step:  $\Phi$  drops dramatically, and the process restarts by focusing on stars with the smallest proper motions; (5) finally, objects that were unpaired in the first step as well as suspicious cases as regards magnitude or position matching are considered, now allowing for periodical jitter. The pipeline converges rapidly; it was shown to be robust in artificial and survey tests, and is also effective in finding binary candidates.

A proper motion catalog was constructed for the 2MASS stars that were present in the PARSEC program fields (Andrei *et al.* 2011). The catalog samples  $42.3 \text{ deg}^2$  of the southern hemisphere, except for the lowest Galactic latitudes where the number of known L/T dwarfs is significantly reduced. It covers the first 18 months of observations, based on independent reduction of each of the eight CCDs of the WFI mosaic using UCAC2 stars. Depending on the number of reference stars, the polynomial degree adopted was 2 or 3, and cross terms were included. The matching criterion used searched for nearest neighbors to 2MASS point sources, with proper motions determined for each observation pair and subsequently averaged while removing deviating values. The resulting rms error is  $5 \text{ mas yr}^{-1}$ , and the correlation with UCAC2 is greater than 0.95. The catalog contains 195,700 entries. Combined with the observed  $z$  and 2MASS magnitudes, this enabled us to obtain reduced proper motions, which we used to select new targets for spectroscopic follow up (Marocco *et al.* 2012).

Determination of parallaxes for BD targets is the central aim of the PARSEC program. To reach a precision of 5 mas or better, this translates to a distance uncertainty of 10% or less; factors of key importance in this context are the degree of coverage of the parallax ellipse, the centroiding method employed, the precision of the astrometric solution, and the solution algorithm used. The first and third issues have already been discussed. The centroiding algorithm was improved for parallax determination using six independent centroid determinations, i.e., those used routinely for TOPP/OATo parallax programs, IRAF's DAOFIND/PHOT, CASU's barycenter find algorithm, SExtractor's

barycenter search and Gaussian settings, and the approach implemented in the *Gaia* GBOT routines. The errors from a comparison of these methods show negligible differences for sufficiently frequently imaged stars, with averages ranging from 4.9 to 7.5 mas. However when all stars are included, larger differences appear, with average errors from 7.1 mas for CASU's centroiding routine (which is optimized for barycentric adjustment) to 27.6 mas for the TOPP method.

The unknowns can be grouped into a linear system of observation equations involving astrometric and instrumental parameters. In the absence of other astronomical knowledge or assumptions, the system linking the measured coordinate ( $x$ ) to the standard coordinate ( $\xi$ ) at a given time ( $t$ ), accounting for proper motion ( $\mu_\xi$ ) and parallax ( $\pi$ ), and mediated by plate constants ( $a, b, c$ ), is rank-deficient:  $\xi_0 + \mu_\xi \Delta t + \pi P_\xi - x - (ax + by + c) = 0$ . Three methods were used to solve for the parallax.

The Two Step Standard Approach Method has been successfully used in the PARSEC and previous OATo parallax programs (Smart *et al.* 2003). A basis frame is defined, usually based on the first well-observed image, since the number of stars is not a limitation given the quality of the instrument and site. The other frames are matched to the basis frame using stars in common to solve for the plate constants. Since the target star is excluded from the sample used for frame adjustment, proper motion and parallax terms are not important (the stars for which they are important are excised from the process). With all standard coordinates converted to the base frame, the astrometric solution can be calculated:  $\xi_t = \xi_{t_0}(1 + a) + \mu_\xi \Delta t + \pi P_\xi$ . The parallax factors are determined from the best available values for the Earth's coordinates. On determining the proper motions and parallaxes, the process can be iterated or the degree of the polynomial adjustment to the basis frame may be increased, but practice shows that this was usually not necessary in the PARSEC program because of the robust instrumental, methodological, and observational setups.

The GAUSSFIT Robust Least-Squares estimation (Bucciarelli *et al.* 2010) constructs a single system of equations, which includes the astrometric parameters of all stars and the instrumental parameters of all frames. The stellar quantities are given in equatorial standard coordinates and instrumental parameters are modeled by a first-order polynomial. The observation equation for a generic star in a given frame is  $-x = ax + by + c - \xi_0 - \mu_\xi \Delta t - \pi P_\xi$  and the parameters to be estimated are  $\xi_0$ ,  $\mu_\xi$ , and  $\pi$ , i.e., the components of the star's position at  $t_0$ , its proper motion and parallax, as well as the instrumental coefficients ( $a, b, c$ ) that map each frame onto the tangential plane. The intrinsic rank deficiency is tackled by employing a direct approach, requiring nine additional constraints to fix the solution. This corresponds to fixing the astrometric parameters relative to the barycenter, which is assumed to be at rest. This way, the approach orthogonalizes the astrometric parameters of the reference stars with respect to the instrumental parameters.

Finally, in the Direct Ellipse Fitting approach, as starting point a mean frame is built using the step-wise polynomial adjustment of frames that were taken close in time and matching is done by hierarchical cone search. Next, the ecliptic standard coordinates ( $\xi_i^e, \eta_i^e$ ) at observation epoch  $t_i$  of the target star are derived. They are fitted by adopting elliptical motion for the parallactic effect, superimposed on a linear term for the transverse motion, i.e.,  $\xi_i^e(x, y) = \xi^e + \pi_\xi \sin(t_i + \Phi_\xi) + \mu_\xi \Delta t$ . Here, the left-hand side is the ecliptic standard coordinate for the observation,  $\xi^e$  is the mean ecliptic standard coordinate,  $\pi_\xi$  and  $\mu_\xi$  are ecliptic components of the parallactic and transverse motions, and  $\Phi_\xi$  is a phase-free term. As for the other methods, there are analogous equations for the  $\eta$  component. The effect of Earth's eccentricity is disregarded, given the typical distances to our targets. It can, in principle, be computed and corrected for, since it is a

**Table 1.** Example of simultaneous solution using the three parallax methods (see text for details) for the high proper-motion star LHS 3482 (2MASS J19462386+3201021), based on 6 years of observations, 93 individual frames, and 54 reference stars.

Method	$\pi$ (mas)	$\mu_{\alpha} \cos \delta$ (mas yr <sup>-1</sup> )	$\mu_{\delta}$ (mas yr <sup>-1</sup> )
Two-Step Standard Approach	68.7 ± 4.0	458.8 ± 1.2	-391.2 ± 2.0
GAUSSFIT Robust Least-Squares	68.9 ± 0.8	457.5 ± 0.2	-390.4 ± 0.3
Direct Ellipse Fitting	70.0 ± 3.2	467.7 ± 0.7	-392.0 ± 1.7

purely geometric effect. Nevertheless, a computation of the differences for three fictitious stars at 20 pc and at ecliptic latitudes  $b = 0^\circ, 45^\circ, 90^\circ$ , sampled from four to nine times during six months covering the span of the year (or of ecliptic longitudes), and adjusted to a parallactic ellipse, shows no contribution to the parallax in excess of  $10^{-8}$  arcsec.

### 3. Selected Results

The average of the parallax error for the first 49 BD targets is 1.7 mas, which corresponds to a typical error of 2.5% in the absolute distances. The full results will be presented in a forthcoming publication. Here we show (see Table 1) a comparison of the three methods to determine the parallaxes. Note that the errors are internal. The Two Steps Standard Approach method exhibits larger errors because it compares results from all stars in the field, while the other two methods do not fully do so. Fig. 1 presents an example of the data leading to the determination of a parallax for a target that has been observed regularly throughout the program; it also shows how the parallaxes here obtained contribute to the determination of the mass–temperature relationship.

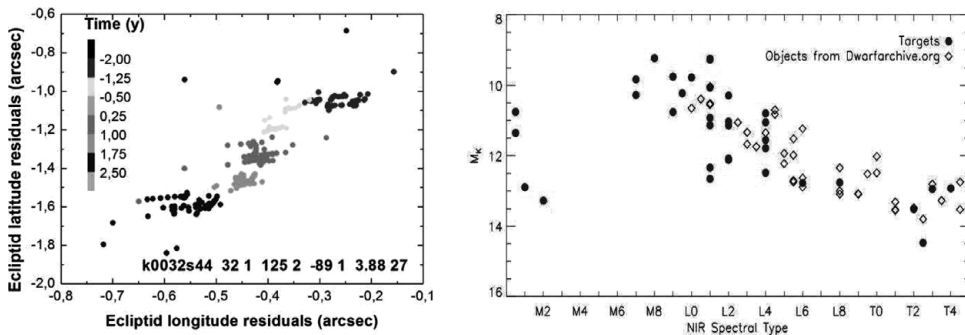


**Figure 1.** (left) The data (residuals of the static solution) leading to derivation of the parallax and proper motion of BD target k0032s44, which was well-sampled throughout the entire PARSEC program. (right) Absolute 2MASS **K** magnitude versus spectral type, where the absolute magnitude was derived from the PARSEC trigonometric parallaxes.

### Acknowledgements

AAH acknowledges support from CNPq grant PQ306775/2009-3 and a PARSEC International Incoming Fellowship of the European Commission’s Marie Curie Seventh Framework Program.

### References

- Andrei, A. H., Smart, R. L., Penna, J. L., *et al.* 2011, *AJ*, 141, 54  
 Bucciarelli, B., Andrei, A. H., Smart, R. L., *et al.* 2010, *Journées Systeme de Reference Space–Temporel 2010*, p. 105  
 Smart, R. L., Lattanzi, M. G., Bucciarelli, B., *et al.* 2003, *A&A*, 404, 317  
 Marocco, F., Andrei, A. H., Smart, R. L., *et al.* 2012, *AJ*, submitted